Towards a picosecond transform-limited nitrogen-vacancy based single photon source

Chun-Hsu Su, Andrew D. Greentree, and Lloyd C. L. Hollenberg

Quantum Communications Victoria, School of Physics,
The University of Melbourne, Victoria 3010, Australia

chsu@ph.unimelb.edu.au

Abstract: We analyze a nitrogen-vacancy (NV^-) colour centre based single photon source based on cavity Purcell enhancement of the zero phonon line and suppression of other transitions. Optimal performance conditions of the cavity-centre system are analyzed using Master equation and quantum trajectory methods. By coupling the centre strongly to a high-finesse optical cavity [$Q \sim \mathscr{O}(10^4 - 10^5)$, $V \sim \lambda^3$] and using sub-picosecond optical excitation the system has striking performance, including effective lifetime of 70 ps, linewidth of 0.01 nm, near unit single photon emission probability and small [$\mathscr{O}(10^{-5})$] multi-photon probability.

OCIS codes: (230.0230) Optical devices; (230.6080) Sources; (160.4760) Optical properties; (160.2220) Defect-center materials

References and links

1. E. S. Polzik, J. Carri, and H. J. Kimble, "Spectroscopy with squeezed light," Phys. Rev. Lett. **68,** 3020–3023 (1992).
2. V. Giovannetti, S. Lloyd, and L. Maccone, "Quantum-enhanced measurements: Beating the standard quantum limit," Science **306,** 1330–1336 (2004).
3. E. Knill, R. Laflamme, and G. J. Milburn, "A scheme for efficient quantum computation with linear optics," Nature (London) **409,** 46–52 (2001).
4. P. Kok, W. J. Munro, K. Nemoto, T. C. Ralph, J. P. Dowling, and G. J. Milburn, "Linear optical quantum computing," Rev. Mod. Phys. **79,** 135–174 (2007).
5. E. Waks, K. Inoue, C. Santori, D. Fattal, J. Vuckovic, G. S. Solomon, and Y. Yamamoto, "Quantum cryptography with a photon turnstile," Nature (London) **420,** 762 (2002).
6. E. Waks, C. Santori, and Y. Yamamoto, "Security aspects of quantum key distribution with sub-Poisson light," Phys. Rev. A **66,** 042315 (2002).
7. A. Kuhn, M. Hennrich, and G. Rempe, "Deterministic single-photon source for distributed quantum networking," Phys. Rev. Lett. **89,** 067901 (2002).
8. J. McKeever, A. Boca, A. D. Boozer, R. Miller, J. R. Buck, A. Buzmich, and H. J. Kimble, "Deterministic generation of single photons from one atom trapped in a cavity, " Science **303,** 1992–1994 (2004).
9. B. Barquié, M. P. A. Jones, J. Dingjan, J. Beugnon, S. Bergamini, Y. Sortais, G. Messin, A. Browaeys, and P. Grangier, "Controlled single-photon emission from a single trapped two-level atom," Science **309,** 454–456 (2005).
10. M. Hijlkema, B. Weber, H. P. Specht, S. C. Webster, A. Kuhn, and G. Rempe, "A single-photon server with just one atom," Nature Physics **3,** 253–255 (2007).
11. M. Keller, B. Lange, K. Hayasaka, W. Lange, and H. Walther, "Continuous generation of single photons with controlled waveform in an ion-trap cavity system," Nature (London) **431,** 1075–1078 (2004).
12. C. Brunel, B. Lounis, Ph. Tamarat, and M. Orrit, "Triggered source of single photons based on controlled single molecule fluorescence," Phys. Rev. Lett. **83,** 2722–2725 (1999).
13. B. Lounis and W. E. Moerner, "Single photons on demand from a single molecule at room temperature," Nature (London) **407,** 491–493 (2000).
14. C. Kurtsiefer, S. Mayer, P. Zarda, and H. Weinfurter, "Stable solid-state source of single-photons," Phys. Rev. Lett. **85,** 290–293 (2000).

15. T. Gaebel, I. Popa, A. Gruber, M. Domhan, F. Jelezko, and J. Wrachtrup, "Stable single-photon source in the near infrared," New J. Phys. **6,** 98 (2004).
16. C. Wang, C. Kurtsiefer, H. Weinfurter, and B. Burchard, "Single photon emission from SiV centres in diamond produced by ion implantation," J. Phys. B: At. Mol. Opt. Phys. **39,** 37–41 (2006).
17. E. Wu, J. R. Rabeau, G. Roger, F. Treussart, H. Zeng, P. Grangier, S. Prawer, and J.-F. Roch, "Room temperature triggered single-photon source in the near infrared," New J. Phys. **9,** 434 (2007).
18. D. Englund, D. Fattal, E. Waks, G. Solomon, B. Zhang, T. Nakaoka, Y. Arakawa, Y. Yamamoto, and J. Vučković, "Controlling the spontaneous emission rate of single quantum dots in a two-dimensional photonic crystal," Phys. Rev. Lett. **95,** 013904 (2005).
19. S. Kako, C. Santori, K. Hoshino, S. Götzinger, Y. Yamamoto, and Y. Arakawa, "A gallium nitride single-photon source operating at 200K," Nature Materials **5,** 887–892 (2006).
20. K. Hennessy, A. Badolato, M. Winger, D. Gerace, M. Atatüre, S. Gulde, S. Fält, E. L. Hu, and A. Imamoğlu, "Quantum nature of a strongly coupled single quantum dot-cavity system," Nature (London) **445,** 896–899 (2007).
21. A. J. Shields, "Semiconductor quantum light sources," Nature Photonics **1,** 215–223 (2007).
22. A. D. Greentree, P. Olivero, M. Draginski, E. Trajkov, J. R. Rabeau, P. Reichart, B. C. Gibson, S. Rubanov, S. T. Huntington, D. N. Jamieson, and S. Prawer, "Critical components for diamond-based quantum coherent devices," J. Phys.: Cond. Matt. **18,** S825–S842 (2006).
23. M. J. Hartmann, F. G. S. L. Brandão, and M. B. Plenio, "Strongly interacting polaritons in coupled arrays of cavities," Nature Physics **2,** 849–855 (2006).
24. A. D. Greentree, C. Tahan, J. H. Cole, and L. C. L. Hollenberg, "Quantum phase transitions of light," Nature Physics **2,** 856–861 (2006).
25. D. G. Angelakis, M. F. Santos, and S. Bose, "Photon-blockade-induced Mott transitions and XY spin models in coupled cavity arrays," Phys. Rev. A **76,** 031805(R) (2007).
26. J. Meijer, B. Burchard, M. Domhan, C. Wittmann, T. Gaebel, I. Popa, F. Jelezko, and J. Wrachtrup, "Generation of single color centers by focused nitrogen implantation," Appl. Phys. Lett. **87,** 261909 (2005).
27. D. N. Jamieson, C. Yang, T. Hopf, S. M. Hearne, C. I. Pakes, S. Prawer, M. Mitic, E. Gauja, S. E. Andreson, F. E. Hudson, A. S. Dzurak, and R. G. Clark, "Controlled shallow single-ion implantation in silicon using an active substrate for sub-20-keV ions," Appl. Phys. Lett. **86,** 202101 (2005).
28. J. R. Rabeau, P. Reichart, G. Tamanyan, D. N. Jamieson, S. Prawer, F. Jelezko, T. Gaebel, I. Popa, M. Domhan, and J. Wrachtrup, "Implantation of labelled single nitrogen vacancy centres in diamond using ^{15}N," Appl. Phys. Lett. **88,** 23113 (2006).
29. J. R. Rabeau, A. Stacey, A. Rabeau, F. Jelezko, I. Mirza, J. Wrachtrup, and S. Prawer, "Single nitrogen vacancy centers in chemical vapor deposited diamond nanocrystals," Nano Letters **7,** 3433–3437 (2007).
30. V. Jacques, E. Wu, F. Grosshans, F. Treussart, P. Grangier, A. Aspect, and J.-F. Roch, "Experimental realization of Wheeler's delayed-choice gedanken experiment," Science **315,** 966–968 (2007).
31. N. B. Manson, J. P. Harrison, and M. J. Sellars, "Nitrogen-vacancy center in diamond: Model of the electronic structure and associated dynamics," Phys. Rev. B **74,** 104303 (2006).
32. A. Beveratos, R. Brouri, T. Gacoin, A. Villing, J.-P. Poizat, and P. Grangier, "Single photon quantum cryptography," Phys. Rev. Lett. **89,** 187901 (2002).
33. R. Alléaume, F. Treussart, G. Messin, Y. Dumeige, J.-F. Roch, A. Beveratos, R. Brouri-Tualle, J.-P. Poizat, and P. Grangier, "Experimental open-air quantum key distribution with a single-photon source," New J. Phys. **6,** 92 (2004).
34. C. K. Hong, Z. Y Ou, and L. Mandel, "Measurement of subpicosecond time intervals between two photons by interference," Phys. Rev. Lett. **59,** 2044–2046 (1987).
35. P. P. Rohde, T. C. Ralph, and M. A. Nielsen, "Optimal photons for quantum-information processing," Phys. Rev. A **72,** 052332 (2005).
36. Q. A. Turchette, C. J. Hood, W. Lange, H. Mabuchi, and H. J. Kimble, "Measurement of conditional phase shifts for quantum logic," Phys. Rev. Lett. **75,** 4710–4713 (1995).
37. L.-M. Duan and H. J. Kimble, "Scalable photonic quantum computation through cavity-assisted interactions," Phys. Rev. Lett. **92,** 127902 (2004).
38. L.-M. Duan, B. Wang, and H. J. Kimble, "Robust quantum gates on neutral atoms with cavity-assisted photon scattering," Phys. Rev. A **72,** 032333 (2005).
39. Y. Akahane, T. Asano, B.-S. Song, and S. Noda, "High-Q photonic nanocavity in a two-dimensional photonic crystal," Nature (London) **425,** 944–947 (2003).
40. B.-S. Song, S. Noda, T. Asano, and Y. Akahane, "Ultra-high-Q photonic double-heterostructure nanocavity," Nature Materials **4,** 207–210 (2005).
41. S. Noda, M. Fujita, and T. Asano, "Spontaneous-emission control by photonic crystals and nanocavities," Nature Photonics **1,** 449–458 (2007).
42. P. Olivero, S. Rubanov, P. Reichart, B. C. Gibson, S. T. Huntington, J. R. Rabeau, A. D. Greentree, J. Salzman, D. Moore, D. N. Jamieson, and S. Prawer, "Ion-beam-assisted lift-off techniques for three-dimensional micromachining of freestanding single-crystal diamond," Advanced Materals (Weinheim, Ger.) **17,** 2427–2430 (2005).

43. S. Tomljenovic-Hanic, M. J. Steel, C. Martijn de Sterke, and J. Salzman, "Diamond based photonic crystal microcavities," Opt. Express **14,** 3556–3562 (2006).
44. J. W. Baldwin, M. Zalalutdinov, T. Feygelson, J. E. Butler, and B. H. Houston, "Fabrication of short-wavelength photonic crystals in wide-band-gap nanocrystalline diamond films," J. Vac. Sci. Technol. B **24,** 50–54 (2006).
45. I. Bayn and J. Salzman, "High-Q photonic crystal nanocavities on diamond for quantum electrodynamics," Eur. Phys. J. Appl. Phys. **37,** 19–24 (2007).
46. C. F. Wang, R. Hanson, D. D. Awschalom, E. L. Hu, T. Feygelson, J. Yang, and J. E. Butler, "Fabrication and characterization of two-dimensional photonic crystal microcavities in nanocrystalline diamond,", Appl. Phys. Lett. **91,** 201112 (2007).
47. G. Davies and M. F. Hamer, "Optical studies of the 1.945eV vibronic band in diamond," Proc. R. Soc. Lond. A: Math. and Phys. Sci. **348,** 285–298 (1976).
48. F. Jelezko, T. Gaebel, I. Popa, A. Gruber, and J.Wrachtrup, "Observation of coherent oscillations in a single electron spin," Phys. Rev. Lett. **92,** 076401 (2004).
49. Ph. Tamarat, N. B. Manson, R. L. McMurtie, A. Nitsovtsev, C. Santori, P. Neumann, T. Gaebel, F. Jelezko, P. Hemmer, and J. Wrachtrup, "The excited state structure of the nitrogen-vacancy center in diamond," http://arxiv.org/abs/cond-mat/0610357 (2006).
50. E. T. Jaynes and F. W. Cummings, "Comparison of quantum and semiclassical radiation theory with application to the beam maser," Proc. IEEE **51,** 89–109 (1963).
51. B. W. Shore and P. L. Knight, "The Jaynes-Cummings model," J. Mod. Opt. **40,** 1195–1238 (1993).
52. C. K. Law and H. J. Kimble, "Deterministic generation of a bit-stream of single-photon pulses," J. Mod. Opt. **44,** 2067–2074 (1997).
53. E. M. Purcell, "Spontaneous emission probabilities at radio frequencies," Phys. Rev. **69,** 681 (1946).
54. S. Haroche and J. M. Raimond, "Radiative properties of Rydberg states in resonant cavities," in *Advances in Atomic and Molecular Physics Vol. XX*, D. Bates and B. Bederson, eds. (Academic, 1985), pp. 350–411.
55. J.-M. Gérard and B. Gayral, "Strong Purcell effector for InAs quantum boxes in three-dimensional solid-state microcavities," J. Lightwave Technol. **17,** 2089–2095 (1999).
56. M. Khanbekyan, D.-G. Welsh, C. Di Fidio, and W. Vogel, "Cavity-assisted spontaneous emission as a single-photon source: Pulse shape and efficiency of one-photon Fock state preparation," http://arxiv.org/abs/0709.2998 (2007).
57. L. Tian and H. J. Carmichael, "Quantum trajectory simulations of the two-state behavior of an optical cavity containing one atom," Phys. Rev. A **46,** R6801–R6804 (1992).
58. H. J. Carmichael, *An Open System Approach to Quantum Optics* (Springer, 1993).
59. Y. Dumeige, F. Treussart, R. Alléaume, T. Gacoin, J.-F. Roch, and P. Grangier, "Photo-induced creaton of nitrogen-related color centers in diamond nanocrystals under femtosecond illumination," J. Lumin. **109,** 61–67 (2004).
60. Ph. Tamarat, T. Gaebel, J. R. Rabeau, M. Khan, A. D. Greentree, H. Wilson, L. C. L. Hollenberg, S. Prawer, P. Hemmer, F. Jelezko, and J. Wrachtrup, "Stark shift control of single optical centres in diamond," Phys. Rev. Lett. **97,** 083002 (2006).
61. A. D. Greentree, J. Salzman, S. Prawer, and L. C. L. Hollenberg, "Quantum gate for Q switching in monolithic photonic-band-gap cavities containing two-level atoms," Phys. Rev. A **73,** 013818 (2006).
62. M. J. Fernée, H. Rubinsztein-Dunlop, and G. J. Milburn, "Improving single-photon sources with Stark tuning," Phys. Rev. A **75,** 043815 (2007).
63. D. E. Chang, A. S. Sørensen, P. R. Hemmer, and M. D. Lukin, "Quantum optics with surface plasmons," Phys. Rev. Lett. **97,** 053002 (2006).

1. Introduction

A source that produces single photons on demand is an invaluable tool for precision optical measurement [1, 2] and is a crucial building block for many quantum computing and communication applications. For an attenuated laser, the number of photons per pulse follows a Poisson distribution and the multi-photon probability becomes negligible only in the limit of small mean photon number at the expense of the single-photon probability. In quantum computing, using single photons to store and transport quantum information is natural as information can be easily encoded and manipulated over photonic degrees of freedom e.g. polarization. In linear optical quantum computing (LOQC) [3, 4], it is straightforward to perform single qubit operations on photons with elementary optical components and projective measurements generate photon-photon interactions. In quantum communication, single photon sources can be used for unconditionally secure quantum key distribution (QKD) protocols [5, 6]. To date, single photon generation has been demonstrated with a variety of single quantum emitters such as

atoms [7–10], ions [11], molecules [12,13], diamond colour centres [14–17] and semiconductor quantum dots [18–21].

Diamond defects hold promise as a platform for solid-state quantum optical and quantum computing applications [22], and for the study of condensed-matter analogues [23–25]. One of the most well-studied systems, garnering much attention lately, is the optically active negatively-charged nitrogen-vacancy defect (NV^- centre). The centre consists of a substitutional nitrogen atom and an adjacent vacancy in the carbon lattice. It forms naturally or may be engineered within a diamond matrix using techniques such as single ion implantation [26–28] or chemical vapour deposition [29]. It has a combination of remarkable properties that render it a suitable single photon source candidate. These include robustness against photobleaching, structural stability at room temperature and demonstrated antibunching, which is the hallmark of a single photon source [14]. The centre has also been used to realize Wheeler's delayed-choice experiment [30]. However, the centre has a relatively long photoluminescence lifetime of 11.6 ns and broad spectral width of 150 nm [31], which is not optimal for daylight or optical fibre operation in QKD [32, 33]. Furthermore, the photons are not time-bandwidth limited (or indistinguishable) for the purpose of LOQC where photon indistinguishability is crucial for Hong-Ou-Mandel interference [34] and hence quantum gates [35].

Preparing the centre in a high-finesse quantum cavity offers a solution to these problems. Cavity quantum electrodynamics has been shown to induce a single-photon Kerr nonlinearity [36] and assist quantum gate operation [37, 38]. Under strong photonic confinement, the quantum emitter (the centre in this case) in the cavity interacts coherently with photon states with the effect of modifying photon-emission dynamics. As a result, we show that the spectral properties of the centre can be improved to fulfill the stringent criteria for quantum information applications. Additionally, the emission can be directed into an application or experiment as desired. A suitable cavity is the planar photonic-band-gap (PBG) cavity that defines an excellent cavity with small mode volume (of order one cubic wavelength) and low loss that provides strong centre-photon coupling [39–41] suitable for our purposes.

Advances in fabrication techniques are nearing the stage where preparing a single crystal diamond with PBG structures using lithography and lift-off [42–46] and placing an individual NV centre in the centre of the cavity using ion implantation techniques may be possible. The latter technique permits locating the centre to achieve full emission enhancement. We note that cavities have been used to enhance the emission of quantum-dots [18, 20] and atoms [10] for photon generation. Our study is made in a similar spirit, but a diamond-based device has the advantages of robustness against the environmental noise combined with simplicity of its setup. Here, without loss of generality, we theoretically study the effects of placing the centre within a high-finesse single-moded diamond PBG cavity. We establish the operation criteria (cavity specification and excitation scheme) for an efficient cavity-centre based single photon source.

2. Theory

A model of an NV^- centre has been proposed as a vibronic system with ground (g) and excited (e) electronic states, each given by a series of vibrational sublevels $|g_i\rangle$ and $|e_j\rangle$ respectively, where i and j label the vibrational states [47]. Its emission spectra consists of several phonon lines iPL, corresponding to the transition $|e_0\rangle - |g_i\rangle$. For simplicity, $|e_0\rangle$ is denoted as $|e\rangle$ from now on. Phononic relaxation of the excited state is much faster than the radiative relaxation to the ground state and the photonic transition probabilities were calculated by Davies and Hamer [47] under the WKB approximation. Because of the rapid phononic transitions, we treat the centre as an atomic system with a single excited state $|e\rangle$ and a ground state with ten sublevels $\{|g_i\rangle\}$ (Fig. 1). The fluorescence from the centre corresponds to a transition from the excited spin triplet state (^3E) to an electron spin triplet ground state (^3A) and the dynamics are

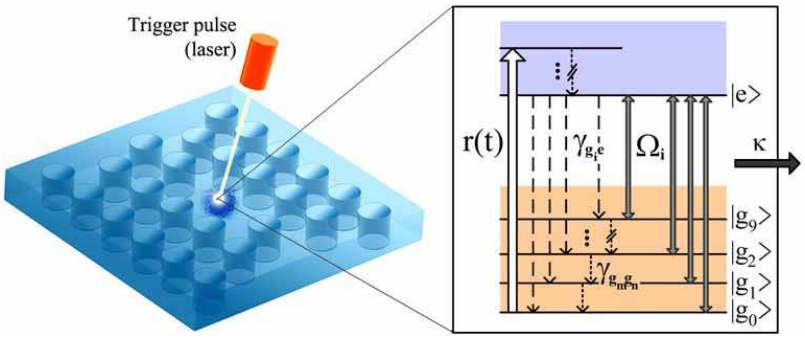

Fig. 1. Theoretical model of a cavity-centre system for single photon generation: the NV centre is modelled as a multi-level atom with a single excited state $|e\rangle$ and a ground state with vibrational sublevels $\{|g_j\rangle\}$. The centre is pumped with an external classical field $r(t)$ (white arrow) acting as the trigger pulse, the transition $|e\rangle - |g_i\rangle$ is coupled to a lossy single-modal cavity with coupling strength Ω_i (grey) and cavity decay rate κ (black). $\gamma_{g_i e}$ (dashed) is the atomic decay rate for radiative transitions $|e\rangle - |g_i\rangle$ while $\gamma_{g_m g_n}$ (dotted) are that for the non-radiative phononic transitions $|g_n\rangle - |g_m\rangle$.

influenced by the presence of a possible metastable state (^1A). We have explicitly ignored the metastable state as its role in de-excitation process remains unclear [31, 48, 49]. Also, in the absence of strain and magnetic field, the transitions from the $m_s = 0$ spin sublevel of the ground state are found to be spin-conserving [31], hence we assume this in our treatment.

To study the transient behaviour of the cavity-centre system, we extend the basic Jaynes-Cummings (JC) model [50, 51], which treats the interaction between a single-mode electromagnetic field or cavity of resonance frequency ω_C and a two-level atom, to consider our more complex atomic system. In the rotating-wave approximation (RWA), the JC Hamiltonian of our cavity-centre system is expressed in terms of the atomic projection operators $\hat{\sigma}_{\alpha\beta} = |\alpha\rangle\langle\beta|$ and the annihilation (creation) operators $\hat{a}$ ($\hat{a}^\dagger$) for single cavity mode as, ($\hbar = 1$)

$$\hat{\mathscr{H}}^{\mathrm{JC}} = \sum_{i=0}^{N_A-2} \omega_{g_i}\hat{\sigma}_{g_i g_i} + \omega_e\hat{\sigma}_{ee} + \omega_C\hat{a}^\dagger\hat{a} + \frac{1}{2}\sum_{i=0}^{N_A-2}(\Omega_i\hat{a}^\dagger\hat{\sigma}_{g_i e} + \mathrm{h.c}), \tag{1}$$

where $N_A = 11$ is the total number of atomic states, ω_α is the energy of the atomic level $|\alpha\rangle$ and Ω_i is the cavity-centre coupling constant between atomic transition $|e\rangle - |g_i\rangle$. In the dipole approximation, the coupling is $\Omega_i = d_i[\omega_C/(2\hbar\varepsilon_0 V)]^{1/2}$ where d_i is the dipole moment of the respective transition. The evolution of the cavity-centre system obeys the Liouville equation of motion for the density matrix ρ,

$$\frac{d\rho}{dt} = -i[\hat{\mathscr{H}}^{\mathrm{JC}},\rho] + \sum_{j=0}^{N_A-2}\gamma_{g_j e}\mathscr{L}[\hat{\sigma}_{g_j e},\rho] + r(t)\mathscr{L}[\hat{\sigma}_{eg_0},\rho] + \sum_{i=0}^{N_A-3}\gamma_{g_i g_{i+1}}\mathscr{L}[\hat{\sigma}_{g_i g_{i+1}},\rho] + \kappa\mathscr{L}[\hat{b}^\dagger\hat{a},\rho], \tag{2}$$

with the Lindbladian terms for some operator $\hat{O}$,

$$\mathscr{L}[\hat{O},\rho] = \hat{O}\rho\hat{O}^\dagger - \frac{1}{2}\left(\hat{O}^\dagger\hat{O}\rho + \rho\hat{O}^\dagger\hat{O}\right). \tag{3}$$

The spontaneous transition ($|e\rangle - |g_j\rangle$) couples to any non-cavity field modes at the characteristic rates $\gamma_{g_j e}$ and non-radiative phononic decays from $|g_{i+1}\rangle$ to $|g_i\rangle$ with rates $\gamma_{g_i g_{i+1}}$. Here $\hat{b}^\dagger$ represents the creation operator for electromagnetic (waveguide) mode outside the cavity,

which the cavity couples to via decay rate κ. The rate $\kappa = \omega_C/(2Q)$ is parameterized by the quality factor of the cavity Q. Incoherent excitation, acting as the trigger for photon emission, is represented by the phenomenological term with a pump absorption rate $r(t)$. In this model, we have explicitly ignored thermal broadening by assuming a zero temperature operating environment. Broadening can be introduced phenomenologically for a more realistic estimate of the linewidth of the emitted wave packet.

Efficient single photon generation requires minimizing loss and fast outcoupling of the excitation via the cavity channel. The appropriate regime to optimise the output is the strong Purcell regime [52], $\kappa > \Omega_i \gg \gamma_{g_j e}$, where the rate of coherent coupling between the centre and cavity mode, Ω_i^2/κ, dominates the rates $\gamma_{g_j e}$ $(\forall j)$ of the incoherent coupling to the non-cavity modes. The cavity mode is chosen to match the transition $|e\rangle - |g_i\rangle$. The cavity loss rate κ sets the time scale for photon outcoupling and when greater than Ω_i, suppresses the vacuum Rabi oscillations, which otherwise lead to unwanted spectral features on the output photon. For a two-level atom in a cavity, altogether embedded in a medium of refractive index n, the enhancement of emission into the cavity is parameterized by the Purcell factor, the ratio of the emission rate to the cavity mode to the unmodified rate into the non-cavity modes [53–55],

$$F_p = \frac{3(\lambda_C/n)^3}{4\pi^2}\frac{Q}{V}, \tag{4}$$

where V is the cavity mode volume and λ_C is the cavity wavelength.

To determine the fraction of pulse cycles that lead to useful output, we must consider the fraction of emitted photons from the atom that enter the desired cavity mode. This fraction is set by the spontaneous coupling factor $\beta = F_p/(1+F_p)$. We demand β to be near unity, which implies a high-Q/V cavity to maximize efficiency, but a small Q for fast cavity loss. These considerations lead to an upper bound for Q, or equivalently, a lower bound on κ given by $\kappa \geq 2\Omega_i$. Beyond this, we enter the strong cavity regime [54]. In this regime, the vacuum Rabi oscillations are not sufficiently suppressed by cavity decay leading to an effective timing jitter or equivalently temporal/spectral features which will degrade overall device performance. Alternatively, if $\kappa < \gamma_{g_j e}$ for large Q, the excitation will be outcoupled as atomic decoherence, which leads to loss of photons through non-guided modes, and manifests as an increased zero photon probability. A rigorous treatment of cavity-assisted emission was made in Ref. [56].

3. Analysis and results

To investigate dynamical processes of photon generation from the cavity-centre system described by Eq. 2, we use direct numerical integration to study the specifications on the trigger pulse that ensures high-fidelity single photon emission and the effect of the cavity on its characteristics. Additionally, we use the quantum trajectory approach to simulate photodetection experiments [57, 58]. We show that it yields results that agree with the former approach and demonstrate bit-stream photon generation and, most importantly, antibunching with the Hanbury-Brown-Twiss (HBT) experiment.

3.1. Determination of the pulsed excitation parameters

The specification of the pulsed excitation scheme for the cavity-centre system is crucial to ensure efficient and high-fidelity single photon emission. The complete treatment of Eq. 2 for this study is computationally demanding as it requires adopting a considerably large state space given by $\{|\alpha\rangle\}_{\text{atomic}} \otimes \{|0_C\rangle, |1_C\rangle, ..., |N_C\rangle\}_{\text{cavity}} \otimes \{|0_W\rangle, |1_W\rangle, ..., |N_W\rangle\}_{\text{waveguide}}$, where the state evolution is taken to span over N_W (or equivalently N_C) excitation states. 'C' denotes the field mode in the cavity and 'W' labels the external waveguide mode. However, for the purposes of understanding just the photon emission, we may reduce the system state space by

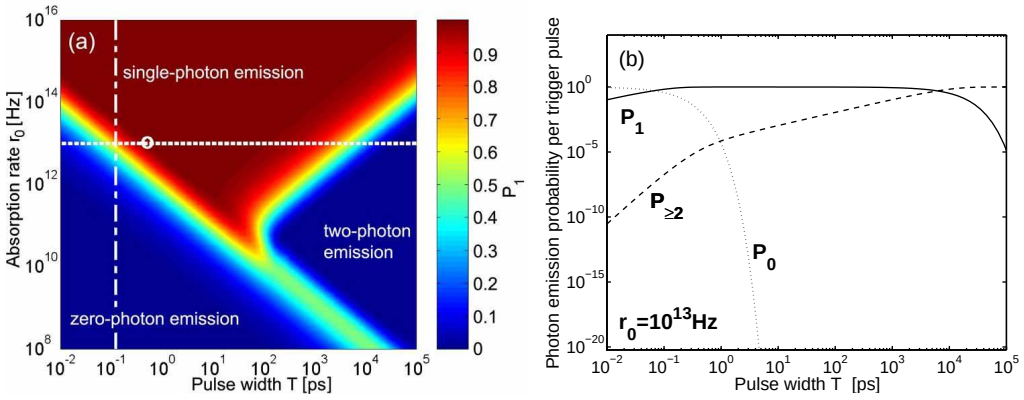

Fig. 2. **a.** Probability of the cavity-centre system ($\omega_C = \omega_{ZPL}, V = \lambda_{ZPL}^3$) to emit a single photon per top-hat excitation pulse as a function of pulse width T and absorption rate r_0. Dash-dotted line denotes the pulse width parameter used in Ref. [59] where the illumination irreversibly transforms the centre into a different centre and is therefore a practical cutoff. Circle labels the parameters [yield $P_1 = 0.996$ and $P_{\geq 2} \sim \mathscr{O}(10^{-5})$] used for the demonstration of single-photon generation with the cavity-centre system. **b.** Zero (dotted), single (solid) and multi- (dashed) photon probability as a function of pulse width with constant absorption rate $r_0 = 10^{13}$ Hz.

setting $N_C = 2$, $N_W = 0$ and enforcing a choice of parameters for the pulsed excitation that limits system population to the ≤ 2-quantum states throughout the cycle.

For the excitation, we assume a top-hat form of the trigger pulse $r(t) = r_0$ for $t \in [0, T]$, where r_0 is the absorption rate and T the pulse width which must be much shorter than the photoluminescence lifetime. In the strong Purcell regime the centre may be approximated as a two-level system in resonance with the cavity, and for very short times we ignore the effects of spontaneous emission and cavity outcoupling. Under these approximations the lower bound for zero photon emission probability (P_0) and the upper bound for one (P_1) are

$$P_0 = \mathrm{e}^{-r_0 T}, \tag{5}$$

$$P_1 = 2\mathrm{e}^{-r_0 T}\left\{\frac{\mathrm{e}^{r_0 T/2}[-16\Omega_i^2 + r_0^2\cosh(\eta T/2)]}{\eta^2} - 1\right\}, \tag{6}$$

and upper bound for multi-photon probabilities is $P_{\geq 2} = 1 - (P_0 + P_1)$, where $\eta = (r_0^2 - 16\Omega_i^2)^{1/2}$. In the limit $r_0 \gg \Omega_i$, Eq. 6 reduces to $P_1 = 1 - \exp(-r_0 T)$, but the second order term reveals that the single photon probability decreases with increasing pulse width according to $\exp(-4\Omega_i^2 T/r_0) - P_0'$, where $P_0' = [2 - \exp(-4\Omega_i^2 T/r_0)]\exp(-r_0 T)$. There is therefore a clear trade-off between the requirement to produce a photon on demand and that of having no more than one photon per pulse. Fig. 2 illustrates the single photon emission probability for an NV centre in a cavity resonant with the zero-phonon line (ZPL) transition ($|e\rangle - |g_0\rangle$), as a function of excitation parameters. In contrast to an attenuated laser where small $P_{\geq 2}$ is achieved in expense of P_1, the cavity-centre system offers $P_1 \sim \mathscr{O}(1)$ while keeping $P_{\geq 2} \leq \mathscr{O}(10^{-2})$. The mean photon number per pulse is $\bar{n} = \sum_i iP_i \approx P_1 + 2P_{\geq 2}$ if P_i is negligible for $i \geq 3$, for these parameter choices.

The photon source must operate in the limit of large r_0 and maintain short T to ensure near unit single photon probability and efficient operation. However, Dumeige *et al.* showed that

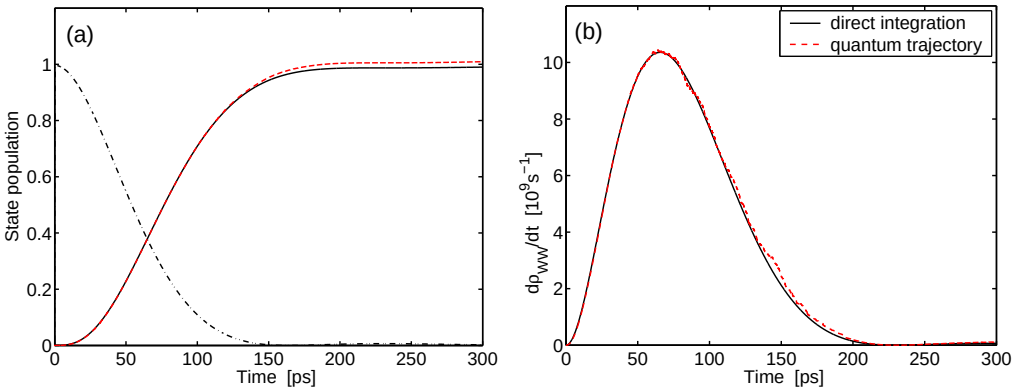

Fig. 3. Evolution of a cavity-centre system ($\omega_C = \omega_{ZPL}$, $V = \lambda_{ZPL}^3$, $\kappa = 2.5\Omega_0$) in response to a top-hat excitation pulse ($r_0 = 10^{13}$ Hz, $T = 0.56$ ps). **a.** Population in $|e,0_C,0_W\rangle$ (the excited centre, black dash-dotted) and $|g_0,0_C,1_W\rangle$ or ρ_{WW} (the outcoupled waveguide mode, black/red solid) as a function of time. **b.** Time derivatives of ρ_{WW}, proportional to the output intensity, with an integrated area of 0.99 (solid) and of 1.01 (dashed red). Simulation is performed by direct integration of Eq. 2 (black solid/dash-dotted) and by quantum trajectory approach as a direct photodetection experiment (red dashed).

under intense femtosecond illumination, the centre becomes photo-ionized, resulting in blinking [59], thus this sets the lower bound for the pulse width.

The optimal excitation parameters for the operation of cavity-centre system depend on the desired application for the photon source. The source can be tailored by varying pulse parameters T and r_0 to optimize properties P_1 and $\overline{n}$ for a specific application. We adopted technically feasible values $T = 0.56$ ps and $r_0 = 10^{13}$ Hz that yield $P_1 = 0.996$ and $P_{\geq 2} = \mathcal{O}(10^{-5})$.

3.2. Simulation of single photon generation with the cavity-centre system

The analysis in Sec. 3.1 allows a determination of the parameter range for single photon emission, and this is obviously the regime in which we want our device to work. In this section, therefore, we work in the single photon emission regime and *assume* single photon output. This affords a considerable saving in computational complexity and we thus truncate the photonic state space to one excitation by setting $N_C = N_W = 1$. We may then solve Eq. 2 numerically to simulate the response of the cavity-centre system to a pulsed excitation, with the result given in Fig. 3. The cavity of volume $V = \lambda_{ZPL}^3$ is chosen to maximize coupling and is in resonance with the ZPL. We choose Q of 36500 so that $\kappa = 2.5\Omega_0$. A photon is being issued at a mean time 70 ps from the pump with excitation outcoupling into the external waveguide mode illustrated by increasing population in $|g_0,0_C,1_W\rangle$ (or $\rho_{WW} \equiv \langle g_0,0_C,1_W|\rho|g_0,0_C,1_W\rangle$). The integral of the derivative $\dot{\rho}_{WW}$ is near unity at 0.99, as required of a single photon pulse. Fourier transform of the temporal profile yields an emission spectrum centered at λ_{ZPL} with effective linewidth of 0.01 nm.

Due to the difference between cavity-centre coupling Ω_0 and cavity outcoupling κ, the resultant photon pulse does not take the form of a Gaussian function which is optimal for LOQC [35]. In principle, Stark tuning [60] can be used to optimize the atom-cavity coupling to reshape the temporal pulse profile [61, 62] and suppress timing jitter. Note that there is a gentle hump at 300 ps, representing the Rabi remnant, that can be eliminated with greater cavity damping.

To simulate photodetection experiments via the quantum trajectory approach, we again adopt

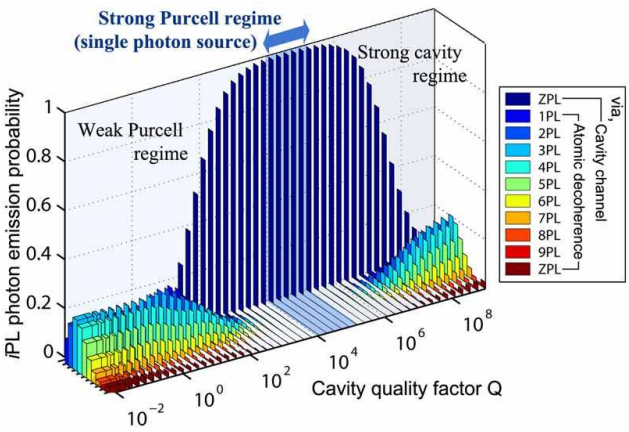

Fig. 4. Comparison of the probability of the cavity-centre system ($\omega_C = \omega_{ZPL}, V = \lambda_{ZPL}^3$) to emit a photon of ω_{ZPL} via the cavity channel and to emit iPL photon via atom decoherence as a function of cavity quality factor Q.

a two-level model of the centre, but truncate $N_C = 4$ to allow for the possibility of multi-photon occupation and subsequent emission. There is a good agreement between this result and that from direct integration, as shown in Fig. 3.

It is instructive to observe how the probability of the system to emit a photon via the cavity and via atomic decoherence varies under the influence of the cavity. We recalculate the emission (Fig. 4), but this time treat (N_A–1) vibrational ground states, and only consider one photonic excitation. In the weak Purcell regime, the excitation is outcoupled via the atomic decoherence channel. The relative transition probabilities of the respective phonon lines jPL approach the unmodified atomic branching ratios $\gamma_{g_j e}$ in the limit of small Q. However, in the strong Purcell regime with $Q \sim \mathcal{O}(10^4 - 10^5)$, the ZPL transition is enhanced by the cavity while other transitions are suppressed accordingly. The excitation is predominantly outcoupled via the cavity relaxation channel, representing the optimal regime for the single-photon source. We note that such Q's are technically achievable and have been demonstrated in Ref. [39, 40] in silicon, and are feasible in diamond [43]. Finally, in the strong cavity regime, the Purcell enhancement diminishes as the time scale for cavity relaxation becomes much longer with $\kappa < \gamma_{g_j e}$.

We have also considered the possibility of enhancing the higher order phonon side bands. Such an enhancement is attractive from the point of view of shifting the emission further into the IR, and taking advantage of the increased dipole moments. The presence of the vibrational sublevels and phononic decays introduces an additional complication to the dynamics of the basic JC model. By explicitly considering a reduced centre model with $|e\rangle$ and $|g_i\rangle$ ($i = 0, 1, 2$ only) that couples the cavity that is in resonance with the 1PL, we have obtained an analytical expression to the modified decay rate by solving the master equation for its eigenfrequencies and assuming $\Omega_0 \ll (\kappa + \gamma_{g_m g_n})$. Single excitation relaxes at an overall damping rate,

$$\gamma_{\text{overall}} = \gamma_{g_0 g_1} + \frac{2\Omega_0^2}{\omega_C/(2Q) + \gamma_{g_m g_n} - 2\gamma_{g_0 g_1}} + \mathcal{O}(\Omega_0^4). \tag{7}$$

Eq. 4 is recovered by setting $\gamma_{g_0 g_1} = \gamma_{g_m g_n} = 0$. The phononic decay reduces the coherence between the states $|g_1, 1_C\rangle$ and $|e, 0_C\rangle$, inhibiting the Purcell enhancement. Hence, to enhance the higher phonon transitions, one requires Ω_0 of order $\mathcal{O}(\gamma_{g_m g_n})$ or a cavity whose modal volume is much smaller than the scale of wavelength^3. Although technically demanding, we note that sub-wavelength confinement may be possible with plasmonic cavities [63].

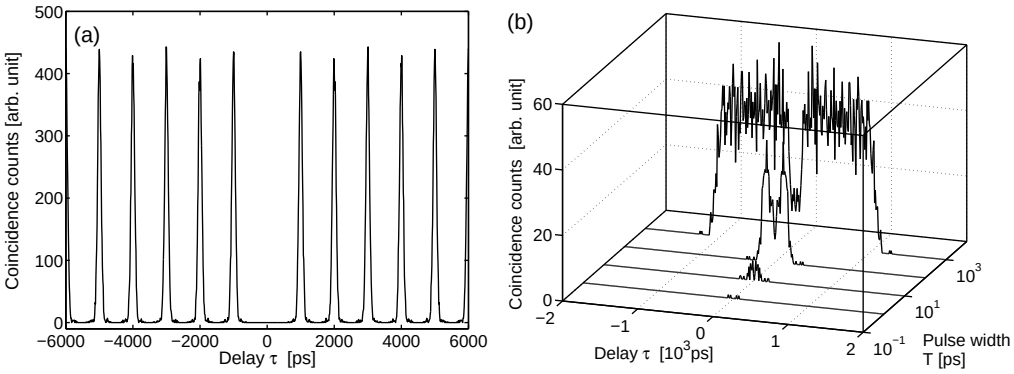

Fig. 5. Photon correlation histogram of emission from the cavity-centre system under pulsed excitation of top-hat functional form obtained using a HBT setup with quantum trajectory approach. The simulations involve **a.** excitation pulse of temporal width $T = 0.56$ ps and constant absorption rate $r_0 = 10^{13}$ Hz at a repetition rate of 1 GHz for a trajectory time of 5 μs, and **b.** excitation pulse of varying temporal widths and constant $r_0 = 10^{13}$ Hz at repetition rate of 0.5 GHz for total time 1.5 ms.

3.3. Antibunching with a HBT setup

Photon correlation obtained from a HBT experiment is a test for single-photon emission. The HBT setup is simulated with a pulsed excitation of rate 1 GHz for a simulation time of 5 μs and the correlation histogram of emission from the cavity-centre system is shown in Fig. 5(a). The experiment assumes the use of a detector with a time bin size of 10 ps. The result shows a series of peaks separated by the clock period of the pulse. The suppression of the coincidences observed at zero delay signifies antibunching. More importantly, the suppression is observed during the period of a single excitation cycle for the short excitation pulse width $T = 0.56$ ps. The single photon probability per excitation trigger, estimated from the ratio of the number of single photon events to total number of pulses simulated is 0.99, while multi-photon probability is zero. With an effective lifetime of 70 ps, the system is capable of operating at an excitation rate of 10 GHz. However, to ensure all photon pulses are well-localized within their respective time bins, a bit-stream rate of 1 GHz is preferable. Finally, in Fig. 5(b), we show an increase in multi-photon probability with increasing excitation pulse width. In agreement with the result from Fig. 2(b), a considerably long simulation is needed to observe an appreciable multi-photon probability of $\mathscr{O}(1)$% for $T \sim 10^3$ ps, the simulation was performed over a trajectory period of 1.5 ms and resolution set to 10 ps.

4. Conclusion

We have studied the effect of a cavity on an NV^- defect centre in enhancing its spectral properties for the purpose of single photon generation for quantum computing and communication. Assuming an atomic-vibronic NV model in single-mode cavity, we have shown that by coupling the centre strongly to a high-Q/V [$Q \sim \mathscr{O}(10^4 - 10^5)$, $V \sim \lambda^3$] cavity that is resonant with the ZPL and with excitation using a sub-picosecond pump, the cavity-centre system is capable of issuing a photon of wavelength 638 nm with high spectral purity. We predict that the cavity-enhanced NV centre can have an effective lifetime of 70 ps and linewidth of 0.01 nm, in contrast with an unmodified centre's photoluminescence lifetime of 11.6ns and spectral width of 150 nm. Photons are emitted with near unit single photon probability of 0.99 while maintaining small multi-photon probability $\mathscr{O}(10^{-5})$, thus making it a relatively efficient triggered

photon source compared to a bare NV centre or an attenuated laser. Finally, the device can potentially operate at a repetition rate of 1 GHz, considerably greater than demonstrated NV systems for QKD applications [32, 33].

Acknowledgments

We thank J. H. Cole and A. M. Stephens for helpful discussions. This project was supported by Quantum Communications Victoria (QCV), which is funded by the Victorian Government's Science, Technology and Innovation (STI) initiative, and by the Australian Research Council (ARC), the Department of Education Science and Technology under the International Science Linkages scheme and the EU 6th Framework under the EQUIND collaboration. ADG is the recipient of an Australian Research Council Queen Elizabeth II Fellowship (project number DP0880466), LCLH is the recipient of an Australian Research Council Australian Professorial Fellowship (project number DP0770715).